Negative pion capture in HD gas and in H_2+D_2 gas mixtures: Resolution of the isotope puzzle

James S. Cohen*

Theoretical Division, Los Alamos National Laboratory, Los Alamos, New Mexico 87545

The cross sections, initial quantum numbers, and kinetic energies for pionic atoms formed by negative pion capture in mixtures of isotopic hydrogen molecules are calculated using the fermion-molecular-dynamics (FMD) method. With these cross sections, the reduced capture ratio for a H_2+D_2 mixture is found to be $(P_p^{(H_2+D_2)}/P_d^{(H_2+D_2)})/(c_p/c_d)=1.204$, and the capture ratio for HD is found to be $P_p^{(HD)}/P_d^{(HD)}=0.875$. In light of these results, the p-to-d pion transfer probabilities Q are reevaluated using prior experimental data and determined to be larger than previously thought: $Q=0.28$ at deuterium fraction $c_d=0.5$ and $Q=0.42$ as $c_d \rightarrow 1$. The puzzling relationship of the experimental data for HD to that for H_2+D_2 mixtures is explained. [S1050-2947(99)06806-7]

PACS number(s): 36.10.−k, 25.80.Gn, 34.10.+x, 34.70.+e

I. INTRODUCTION

Stopping of negative pions and muons in mixtures of hydrogen and deuterium has been studied for many years, but the behavior has not been well understood. In particular, the essential first step, capture of the negative particle by displacement of a target electron, has not previously been treated theoretically with *molecular targets*. Over a decade ago, calculations [1] with *atomic targets* showed that H atoms are slightly more likely than D atoms to capture the negative particle, due almost completely to the reduced-mass effect; in an equimolar mixture, the fraction of μ^- captured by H was found to be 51.6%. However, experiments with pions show that there is a substantial difference between capture by HD molecules [2] and capture in an equimolar H_2+D_2 mixture [2–5], thus demonstrating that molecular effects are important.

For many purposes in atomic physics, negative muons (μ^-) and pions (π^-), which have similar masses ($m_\mu=206.77m_e$ and $m_\pi=273.14m_e$), behave similarly. This is true for initial capture by atomic or molecular targets, and for isotopic transfer from a given n,l level. However, in most experiments the two particles behave quite differently since the π^- is usually absorbed by the nucleus via the strong interaction before reaching the ground $1s$ state, while the weakly interacting μ^- is likely to reach the ground state. In fact, the probability, denoted q_{1s}, that a μ^- reaches the ground state of the lighter isotope in a mixture before being transferred is an important quantity in muon-catalyzed fusion; however, μ^- transfer in excited states is difficult to determine experimentally (though recent developments with charge-coupled devices have made it possible [6]). In this regard, pions offer two advantages.

(i) A distinctive diagnostic due to the nuclear charge-exchange reaction,

$$p\pi^- \rightarrow n\pi^0 \text{ followed by } \pi^0 \rightarrow \gamma\gamma, \qquad (1)$$

with branching ratio $\sim 60\%$ [7], which is strongly sup-

pressed (by $\sim 10^4$) in $d\pi$ [8]. Thus *coincident* γ's uniquely identify capture on a proton. (The other 40% of $p\pi$ atoms undergo the reaction $p\pi \rightarrow \gamma n$, which is similar to the reaction $d\pi \rightarrow \gamma nn$, both of which yield a single high energy γ.)

(ii) Expectation that the π^- transfer (for the pions that subsequently nuclear capture on the deuteron) occurs at levels $n=4$ or 5 since external Auger deexcitation (usually with $\Delta n=-1$) dominates at higher n and nuclear capture dominates at lower n [9,4].

Experiments with μ^- rely on radiative decay x rays, which are subject to greater background and small isotope shifts, as a diagnostic and are usually done on a time scale too slow to distinguish excited-state transfer.

Given the seeming simplicity of the hydrogen molecule target, one might well wonder why the relevant theory has not been carried out before. Actually, even the atomic hydrogen target is not easily treated by standard quantum-mechanical methods since the electronic continuum and a large number of pionic bound states must be included. The molecular target is much more difficult since the rotational and vibrational degrees of freedom need to be explicitly treated. The quasiclassical fermion-molecular-dynamics (FMD) method has recently been applied to $\bar{p}$ and μ^- [10,11] capture by the molecules H_2 and D_2, with rather surprising results. It was found that molecular effects, mainly vibrational excitation and predissociation, enable capture by molecules to reach much higher collision energies than does capture by atoms, whose cross sections fall rapidly at energies exceeding the target ionization threshold [12,13]. The molecular effects were found to be most important for the closest projectile–target nucleus mass match, as in $\bar{p}+H_2$, but to still be quite significant in cases like μ^-+D_2. The FMD method has also been validated for μ^- capture by the hydrogen *atom* [14] by comparison with an accurate quantum-mechanical calculation [15].

In the present paper, the FMD method is applied to π^- capture by the H_2 and D_2 molecules as well as the isotopic molecule HD. Once the π^- is captured by H_2 or D_2 one can be confident that a $p\pi$ or $d\pi$ atom, respectively, will result (since nuclear charge exchange from a large mesomolecular orbital [16] or cascade to a low mesomolecular orbital with-

out dissociation are both improbable). The treatments of the molecular capture and dissociation dynamics are unified in the FMD description. Normally the dissociation time scale is significantly longer than the time scale of the initial capture, which usually is accompanied by ejection of an electron. Generally, the velocity of this electron is much higher than the velocities of the heavier particles.

In π^- capture in a dense gas, a number of steps may occur: (a) slowing down, (b) molecular capture, (c) dissociation to pionic atom, (d) atomic cascade/thermalization, (e) isotopic transfer, and (f) nuclear reaction. Our present calculations show that the molecular capture cross sections in step b are significantly different for H_2, D_2, and HD, *and* that the dissociation of $pd\pi$ in step c is significantly asymmetric. With the resulting capture fractions, different transfer probabilities are deduced, and it is no longer necessary to assume theoretically anomalous molecular or isotopic effects in steps d–f in order to interpret the experimental data. A consistent picture of π^- capture in HD gas and the H_2+D_2 mixture then emerges.

II. FERMION MOLECULAR DYNAMICS

The FMD method [17] enables approximate description of the dynamics of quantum-mechanical systems via solution of classical equations of motion. This leap is achieved using constraining potentials to prevent the system from occupying quantum-mechanically forbidden (by the Heisenberg or Pauli principles) regions of phase space. The basic idea is to simulate this quantal reality without affecting the dynamics in regions where the motions are nearly classical. The formulation of the FMD method for collisions of charged particles with the hydrogen molecule has previously been described in detail [10]. The only difference in the present application is that an asymmetric target, the isotopic HD molecule, is also treated. Other than the mass in the Hamiltonian, there is no change in the equations solved. For this problem the FMD method solves Hamilton's classical equations of motion,

$$\dot{\mathbf{r}} = \nabla_{\mathbf{p}} H_{\mathrm{FMD}}, \tag{2a}$$

$$\dot{\mathbf{p}} = -\nabla_{\mathbf{r}} H_{\mathrm{FMD}}, \tag{2b}$$

in terms of the laboratory-frame variables, $\mathbf{r} = \{\mathbf{r}_a, \mathbf{r}_b, \mathbf{r}_c, \mathbf{r}_1, \mathbf{r}_2\}$ and $\mathbf{p} = \{\mathbf{p}_a, \mathbf{p}_b, \mathbf{p}_c, \mathbf{p}_1, \mathbf{p}_2\}$, where subscript a tags the incident π^-, subscripts b and c tag the target nuclei (p or d), and subscripts 1 and 2 tag the target electrons. In addition, the following definitions are employed: the relative distance

$$\mathbf{r}_{\alpha\beta} \equiv \mathbf{r}_\beta - \mathbf{r}_\alpha, \tag{3}$$

the reduced mass

$$\mu_{\alpha\beta} \equiv \frac{m_\alpha m_\beta}{m_\alpha + m_\beta}, \tag{4}$$

and the relative momentum

$$\mathbf{p}_{\alpha\beta} \equiv \frac{m_\alpha \mathbf{p}_\beta - m_\beta \mathbf{p}_\alpha}{m_\alpha + m_\beta} = \mu_{\alpha\beta} \left(\frac{\mathbf{p}_\beta}{m_\beta} - \frac{\mathbf{p}_\alpha}{m_\alpha} \right). \tag{5}$$

In these definitions a value of ''o'' for α or β implies the quasiparticle values [10],

$$m_o = m_b + m_c, \tag{6}$$

$$\mathbf{r}_o = \tfrac{1}{2}(\mathbf{r}_1 + \mathbf{r}_2), \tag{7}$$

and

$$\mathbf{p}_o = \mathbf{p}_1 + \mathbf{p}_2. \tag{8}$$

The FMD effective Hamiltonian is written

$$H_{\mathrm{FMD}} = H_0 + V_{\mathrm{pseudo}}, \tag{9}$$

where H_0 is the usual Hamiltonian for the five-body system (consisting of particle kinetic energies and pairwise Coulomb potentials) and V_{pseudo} is a pseudopotential introduced in the FMD formulation to prevent classical collapse of the many-body system. The FMD method achieves this stabilization with [10]

$$V_{\mathrm{pseudo}} = V_H + V_P + V_{m1} + V_{m2}, \tag{10}$$

where

$$V_H = \frac{1}{\mu_{b1} r_{b1}^2} f(r_{b1} p_{b1}; \xi_H) + \frac{1}{\mu_{c1} r_{c1}^2} f(r_{c1} p_{c1}; \xi_H)$$
$$+ \frac{1}{\mu_{b2} r_{b2}^2} f(r_{b2} p_{b2}; \xi_H) + \frac{1}{\mu_{c2} r_{c2}^2} f(r_{c2} p_{c2}; \xi_H)$$
$$+ \frac{1}{\mu_{ba} r_{ba}^2} f(r_{ba} p_{ba}; \xi_H) + \frac{1}{\mu_{ca} r_{ca}^2} f(r_{ca} p_{ca}; \xi_H),$$
$$\tag{11}$$

$$V_P = \frac{1}{\mu_{12} r_{12}^2} f(r_{12} p_{12}; \xi_P) \delta_{s_1, s_2}, \tag{12}$$
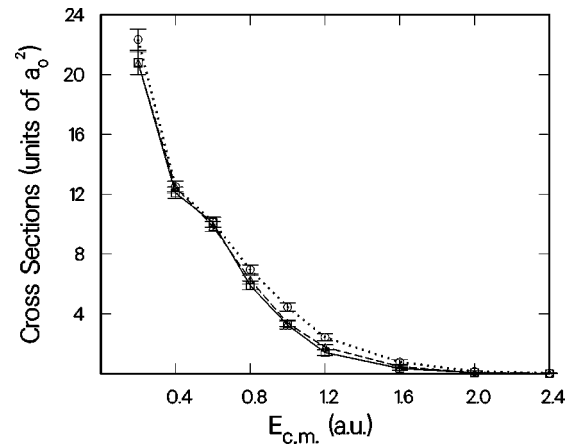
FIG. 1. Initial total capture cross sections for π^- in collisions with H_2 (circles joined by dotted curve), D_2 (squares joined by solid curve), and HD (triangles joined by dashed curve). The error bars are statistical, one standard deviation.

TABLE I. Energy-dependent cross sections and parameters of the n and l distributions for $p\pi$ atoms formed in $\pi^- + H_2$ collisions. $\sigma_{p\pi}^{(H_2)}$ is the $p\pi$-formation cross section and $\sigma_{tot}^{(H_2)}$ is the total inelastic cross section. The n distributions $F_n(n;E)$ have peaks at n_0 and half widths γ; details of the fits and behavior at small and large n are given in Appendix A of Ref. [10]. [Note the following errata in Ref. [10]: in Eq. (A4), δ should be γ; in Eq. (A15), c should be c_1 on the first line and c_2 on the second line.] The l distributions $F_1(l;E)$ are fit by $c(2l+1)\exp(bl^2)\exp[-al^2/(l_1-l)^2]$, where c is a normalization constant; see Appendix B of Ref. [10] for details.

$E_{c.m.}$ (a.u.)	$\sigma_{p\pi}^{(H_2)}$ (in a_0^2)	$\sigma_{tot}^{(H_2)}$ (in a_0^2)	n_0	γ	b	a	l_1
0.01	158.90 ± 4.88	158.90 ± 4.88	12.13	1.12	-8.73×10^{-3}	1.76×10^{-2}	12
0.10	35.34 ± 1.30	35.34 ± 1.30	11.78	2.21	-1.59×10^{-4}	6.48×10^{-2}	14
0.20	22.34 ± 0.71	22.45 ± 0.71	12.31	2.11	-7.67×10^{-3}	3.26×10^{-2}	16
0.40	12.51 ± 0.35	15.41 ± 0.51	13.65	2.81	-1.11×10^{-2}	1.43×10^{-2}	19
0.60	10.14 ± 0.33	12.58 ± 0.44	15.63	4.58	-6.63×10^{-3}	3.61×10^{-4}	26
0.80	6.96 ± 0.31	11.38 ± 0.48	15.52	3.54	-4.51×10^{-3}	1.15×10^{-4}	35
1.00	4.45 ± 0.28	10.57 ± 0.51	17.18	4.68	5.97×10^{-3}	$2.44 \times 10^{+0}$	37
1.20	2.44 ± 0.24	9.90 ± 0.51	20.03	5.34	4.29×10^{-3}	$1.50 \times 10^{+0}$	39
1.60	0.78 ± 0.16	9.19 ± 0.47	16.36	0.64	1.80×10^{-2}	$1.10 \times 10^{+1}$	43
2.00	0.14 ± 0.07	9.01 ± 0.45	[a]				
2.40	0.03 ± 0.03	9.22 ± 0.47					

[a]There were not enough trajectories forming the exotic atom at the higher energies to allow reliable fits of the quantum-number distributions.

$$V_{m1} = \frac{1}{\mu_{o1}r_{bc}^2}f(r_{o1}p_{o1};\xi_{m1}) + \frac{1}{\mu_{o2}r_{bc}^2}f(r_{o2}p_{o2};\xi_{m1})$$

$$+ \frac{1}{\mu_{oa}r_{bc}^2}f(r_{oa}p_{oa};\xi_{m1}), \tag{13}$$

and

$$V_{m2} = \frac{1}{\mu_{12}r_{bc}^2}f(r_{12}p_{12};\xi_{m2}), \tag{14}$$

in terms of a repulsive constraining function f. The exact form of f is not important, but with the choice

$$f(rp;\xi) \equiv \frac{(\xi\hbar)^2}{4\alpha}\exp\left\{\alpha\left[1 - \left(\frac{rp}{\xi\hbar}\right)^4\right]\right\} \tag{15}$$

and the hardness constant $\alpha = 4.0$, which is also largely ar-

bitrary, the parameters are $\xi_H = 0.9428$, $\xi_P = 2.609$, $\xi_{m1} = 0.90$, and $\xi_{m2} = 1.73$. It has been shown in previous work that these parameters yield energies for the hydrogen molecule [10] and all atoms [18,19] of the periodic table sufficiently accurate to be useful for some rearrangement collisions that are not tractable by available quantum-mechanical methods. The term V_P vanishes in the present case since the two electron-spin projections, s_1 and s_2, are opposite.

The initial conditions of the target molecule [10] are set by performing a random Euler rotation of the target particles as a rigid body with Cartesian coordinates $\mathbf{r}_b^{(0)} = -\mathbf{r}_c^{(0)} = (0,0,0.6955)$, $\mathbf{r}_1^{(0)} = -\mathbf{r}_2^{(0)} = (0.8714,0,0.3283)$, $\mathbf{p}_b^{(0)} = -\mathbf{p}_c^{(0)} = (0,0,0)$, and $\mathbf{p}_1^{(0)} = -\mathbf{p}_2^{(0)} = (1.0331,0,0)$ in atomic units. The π^- was started at a distance $10a_0$ away (except at the lowest energy, where the initial distance was increased to $20a_0$). In most cases the trajectory could be followed long enough that the product $p\pi$ or $d\pi$, with quasiclassical bins for quantum numbers, could be clearly identified. The cross section for a reaction R is given by

TABLE II. Energy-dependent cross sections and parameters of the n and l distributions for $d\pi$ atoms formed in $\pi^- + D_2$ collisions.

$E_{c.m.}$ (a.u.)	$\sigma_{d\pi}^{(D_2)}$ (in a_0^2)	$\sigma_{tot}^{(D_2)}$ (in a_0^2)	n_0	γ	b	a	l_1
0.01	152.12 ± 5.49	152.12 ± 5.49	11.59	2.04	-6.48×10^{-4}	7.54×10^{-2}	13
0.10	33.07 ± 1.45	33.07 ± 1.45	11.64	2.28	-4.71×10^{-3}	3.39×10^{-2}	15
0.20	20.82 ± 0.80	21.03 ± 0.80	12.61	2.43	2.44×10^{-4}	9.55×10^{-2}	17
0.40	12.09 ± 0.39	13.61 ± 0.47	14.39	3.43	-1.37×10^{-4}	1.72×10^{-1}	20
0.60	10.11 ± 0.35	11.38 ± 0.40	16.48	4.49	-6.69×10^{-3}	6.68×10^{-4}	26
0.80	5.90 ± 0.30	10.57 ± 0.49	17.14	4.58	-4.78×10^{-3}	1.70×10^{-6}	37
1.00	3.25 ± 0.27	9.72 ± 0.51	20.76	7.95	1.75×10^{-4}	8.58×10^{-1}	39
1.20	1.41 ± 0.20	9.12 ± 0.49	18.20	3.65	1.02×10^{-2}	$6.40 \times 10^{+0}$	47
1.60	0.35 ± 0.11	8.76 ± 0.47					
2.00	0.07 ± 0.05	7.95 ± 0.44					

TABLE III. Energy-dependent cross sections and parameters of the n and l distributions for $p\pi$ atoms formed in $\pi^- + HD$ collisions.

$E_{c.m.}$ (a.u.)	$\sigma_{p\pi}^{(HD)}$ (in a_0^2)	$\sigma_{tot}^{(HD)}$ (in a_0^2)	n_0	γ	b	a	l_1
0.01	82.56±3.05	153.92±4.11	12.11	2.27	-1.52×10^{-3}	1.88×10^{-1}	14
0.10	16.68±0.89	32.09±1.25	11.51	2.22	1.62×10^{-4}	2.46×10^{-1}	16
0.20	9.71±0.53	21.08±0.76	12.22	2.27	-3.14×10^{-3}	1.82×10^{-1}	18
0.40	5.39±0.26	14.56±0.45	13.76	2.98	-6.59×10^{-3}	7.23×10^{-2}	20
0.60	4.52±0.24	12.00±0.39	15.58	4.16	-5.72×10^{-3}	1.13×10^{-4}	29
0.80	2.88±0.19	10.67±0.39	16.55	5.21	-4.25×10^{-4}	$1.17\times10^{+0}$	40
1.00	1.64±0.15	10.12±0.39	20.63	8.26	2.56×10^{-3}	$1.91\times10^{+0}$	42
1.20	0.83±0.11	9.42±0.38	18.48	5.55	4.96×10^{-3}	$3.11\times10^{+0}$	44
1.60	0.21±0.06	9.24±0.37					
2.00	0.04±0.02	9.10±0.23					

$$\sigma_R = \sum_i \frac{N_i^{(R)}}{N_i^{tot}} \pi[(b_i)^2 - (b_{i-1})^2], \qquad (16)$$

where $N_i^{(R)}$ of N_i^{tot} trajectories with impact parameter in (b_{i-1}, b_i) yielded reaction R. For $\pi^- + H_2$ and $\pi^- + D_2$, up to 200 trajectories were run in each range of impact parameters to achieve the target precision. For $\pi^- + HD$, this number was increased to 400 (1000 for $E \geq 2.0$ a.u.) in order to obtain a more accurate $p\pi/d\pi$ branching ratio. At $E > 0.1$ a.u., $b_1 = 1.5a_0$ was used; at $E = 0.1$ a.u., $b_1 = 3.0a_0$ and at $E = 0.01$ a.u., $b_1 = 6.0a_0$. Higher ranges of impact parameter were taken with $b_{i+1} = \sqrt{2}b_i$ until convergence was achieved.

III. RESULTS

A. Initial capture — cross sections and distributions

The cross sections for π^- capture by the H_2, D_2, and HD molecules are shown in Fig. 1 and Tables I–IV. The cross sections for $\pi^- + H_2$ and $\pi^- + D_2$ are similar to those for the slightly lighter μ^- [11]. In keeping with the interpretation previously given [11], the cross section for the reaction with the better mass match ($m_\pi/m_p = 0.149$ as compared with $m_\pi/m_d = 0.074$) is relatively larger, especially at the higher energies of capture. This is because the closer mass match enhances vibrational and rotational excitation of the target.

The cross section for $\pi^- + HD$ lies in between those for H_2 and D_2. The small dipole moment of HD apparently is not important to the capture dynamics, except possibly at extremely low collision energies. It is curious that the HD cross section seems to lie closer to that for D_2 than to that for H_2. This observation may be relevant to capture by more complex molecular hydrides.

The total cross section for HD, shown in Fig. 1, reflects the dynamics of the initial large mesomolecular orbital [16]. The subsequent dynamics leading to an atomic orbital and dissociation into either $p\pi$ or $d\pi$ is also essential for comparison with experimental observations. The separate cross sections for $p\pi$ and $d\pi$ are shown in Fig. 2 and in Tables III and IV, respectively. The cross section for forming $d\pi$ is the larger except at $E \lesssim 0.1$ a.u., where the two cross sections appear to cross. The favoring of the heavier isotope might be expected owing to its larger binding energy. At very low energies it is possible the binding effect is counteracted by the long-range interaction with the weak dipole moment tending to orient the target molecule so the incident π^- attaches to the proton first.

The distributions of principal quantum number of the pionic atoms formed, after dissociation of the target molecule and autoionization of any residual electron, are shown in Fig. 3. The quantum number is identified with the quasiclassical binding energy using the relation,

TABLE IV. Energy-dependent cross sections and parameters of the n and l distributions for $d\pi$ atoms formed in $\pi^- + HD$ collisions.

$E_{c.m.}$ (a.u.)	$\sigma_{d\pi}^{(HD)}$ (in a_0^2)	$\sigma_{tot}^{(HD)}$ (in a_0^2)	n_0	γ	b	a	l_1
0.01	71.37±2.76	153.92±4.11	12.00	1.70	-7.16×10^{-3}	5.37×10^{-2}	13
0.10	15.41±0.88	32.09±1.25	11.85	2.36	8.85×10^{-4}	1.40×10^{-1}	15
0.20	11.06±0.54	21.08±0.76	12.70	2.32	-6.06×10^{-3}	4.94×10^{-2}	17
0.40	7.09±0.29	14.56±0.45	14.38	2.99	-6.22×10^{-3}	4.23×10^{-2}	19
0.60	5.32±0.24	12.00±0.39	16.18	3.97	-6.46×10^{-3}	6.65×10^{-4}	27
0.80	3.39±0.20	10.67±0.39	15.61	3.04	-5.24×10^{-3}	1.28×10^{-6}	33
1.00	1.73±0.15	10.12±0.39	17.62	3.65	2.40×10^{-3}	$1.33\times10^{+0}$	37
1.20	0.94±0.12	9.42±0.38	22.29	7.33	2.60×10^{-3}	$1.18\times10^{+0}$	39
1.60	0.27±0.07	9.24±0.37					
2.00	0.05±0.02	9.10±0.23					
2.40	0.01±0.01	8.53±0.22					

FIG. 2. Cross sections for formation of $p\pi$ (dotted curve), $d\pi$ (dashed curve), and their sum (solid curve) in collisions of π^- with HD.

$$n = [(\mu_{ab}/2E_{\text{bind}})^{1/2} + 0.5], \qquad (17)$$

where the brackets $[\ldots]$ designate the greatest integer function. This is the initial quantum number, i.e., before radiation or interactions with any other molecules in the gas occur. Rigorously the initial distribution for a π^- stopped in dense gas is given by the integration,

$$P_n(n) = \int F_n(n;E) \frac{\sigma_{\text{capt}}(E)}{\sigma_{\text{tot}}(E)} F_{\text{arr}}(E) dE, \qquad (18)$$

where $F_n(n;E)$ is the distribution at a given collision energy and $F_{\text{arr}}(E)$ is the "arrival function" [20]. The $F_n(n;E)$ are given at discrete energies, where the FMD calculations were performed, in Tables I–IV. Calculation of the arrival function would require solution of an integral equation involving the slowing-down cross sections, with initial condition for the π^- at an energy much higher than where it is captured. However, previous work has shown that the arrival function tends to be rather flat at the energies where capture occurs
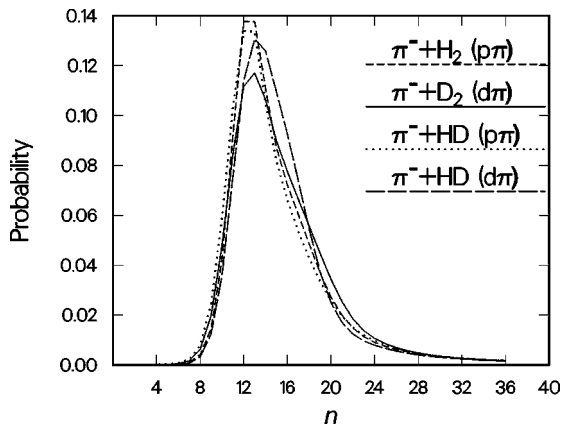
FIG. 3. Normalized distributions of principal quantum number n for $p\pi$ and $d\pi$ atoms formed in collisions of π^- with H_2, D_2, and HD under dense-gas conditions (such that the pion undergoes multiple collisions and is stopped in the target). The points at integral n are joined by straight line segments. These distributions are obtained by integrating the energy-dependent n distributions over the capture cross sections assuming a flat arrival function.
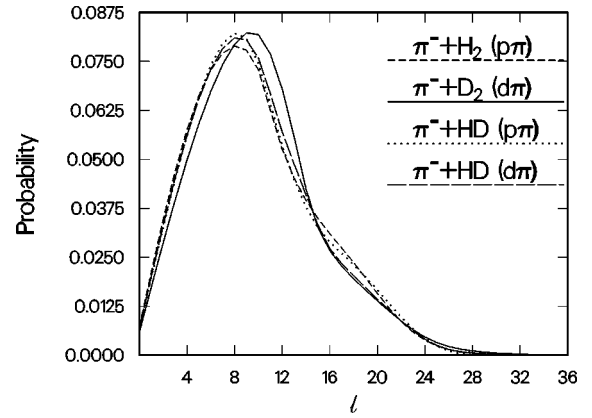
FIG. 4. Normalized distributions of angular-momentum quantum number l for $p\pi$ and $d\pi$ atoms formed in collisions of π^- with H_2, D_2, and HD under dense-gas conditions. The points at integral l are joined by straight-line segments. These distributions are obtained by integrating the energy-dependent l distributions over the capture cross sections assuming a flat arrival function.

(see Fig. 9 of Ref. [12]), and we have approximated it as constant. The main condition for flatness is that the energies where capture occurs not exceed the energy steps in the slowing-down process; as long as this is true, it is not necessary that the capture thresholds be similar. In Fig. 3, it can be seen that the resulting $P_n(n)$ distributions are very similar to each other, peaking at $n \approx 12$ or 13, slightly lower for $p\pi$ than for $d\pi$.

The distributions of initial angular-momentum quantum number l, calculated with analogous approximations, are shown in Fig. 4. The four distributions are again very similar to each other, peaking at $l \approx 8 - 10$.

We have also examined the initial kinetic energies of the pionic atoms. Based on experimental evidence [21–23], it is believed that nonthermal kinetic energies are essential to describing the cascade of pionic atoms. This energy can also come from subsequent Coulomb deexcitation in superelastic collisions, but it is still of interest to know the energies that the atoms start with at large n. These energy distributions are shown in Fig. 5 for the $p\pi$ and $d\pi$ atoms formed in H_2, D_2, or HD gas. As expected, the largest kinetic energies are taken
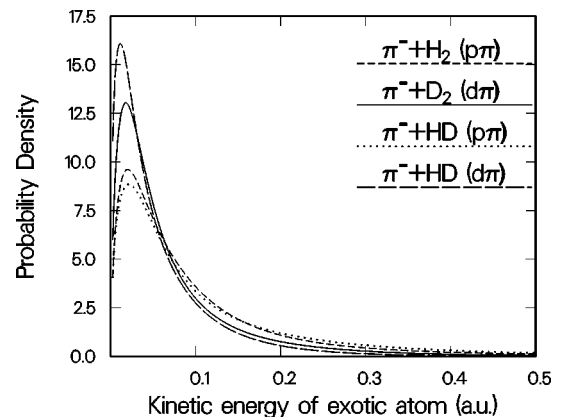
FIG. 5. Initial kinetic-energy distributions (normalized to unity with energy in a.u.) in the laboratory system of the $p\pi$ and $d\pi$ atoms formed by π^- stopped in dense H_2, D_2, and HD targets. See Figs. 3 and 4 for the corresponding internal quantum numbers.

by the lighter exotic atom recoiling from the heavier nucleus. For $\pi^- + H_2$, the distribution peaks at ~ 0.5 eV and has a tail that extends to ~ 10 eV. The tail of the distribution is due to the dissociation dynamics, which is akin to Coulomb deexcitation in collisions.

B. Relative capture in mixtures

With the assumption of a flat arrival function, discussed above, the probability of capture by component i in a binary mixture is

$$P_i = N \int_0^\infty \frac{c_i \sigma_{\text{capt}}^{(i)}(E_{\text{lab}})}{c_1 \sigma_{\text{tot}}^{(1)}(E_{\text{lab}}) + c_2 \sigma_{\text{tot}}^{(2)}(E_{\text{lab}})} dE_{\text{lab}}, \qquad (19)$$

where c_1 and c_2 are the fractions of each species ($c_1 + c_2 = 1$) and N is a normalization constant such that $P_1 + P_2 = 1$ (the generalization to a mixture with more than two components is straightforward). The formula for relative production of $p\pi$ and $d\pi$ in pure HD is similar except only $c_1 = c_2 = 0.5$ is possible.

Equation (19) would seem to suggest a nontrivial dependence of relative capture on c_1 and c_2, and indeed such could be the case for cross sections that have an arbitrary dependence on energy. However, we find in the present case, and perhaps in most physical situations, that the intuitively expected relation $P_1/P_2 \propto c_1/c_2$ (proportionality, not equality) obtains to a good approximation.[1] This is a better approximation than it might seem. A simple analysis suffices to show that the proportionality will hold as long as the energy dependence of the total (slowing-down + capture) cross sections is weak *or* the total cross sections of the two species are similar, *even if the capture thresholds of the two components are quite different.*

The fractions of π^- initially forming $p\pi$ in the $H_2 + D_2$ mixtures are calculated by Eq. (19) with the results shown in Fig. 6. Consistent with the greater cross section for H_2, shown in Fig. 1, $P_p^{(H_2+D_2)}/P_d^{(H_2+D_2)} > c_p/c_d$. As shown, this distribution is fit to an excellent approximation by $(P_p^{(H_2+D_2)}/P_d^{(H_2+D_2)})/(c_p/c_d) = 1.204$ for all c_d, or equivalently

$$P_p^{(H_2+D_2)} = \frac{1}{1 + \alpha C}, \qquad (20)$$

where $C \equiv c_d/c_p$ and $\alpha = 0.83$.

The fraction of π^- initially forming $p\pi$ in pure HD gas is also shown, as a single point ($c_p = c_d = 0.5$), in Fig. 6. In this case, $P_p^{(HD)}/P_d^{(HD)} = 0.875$ or $P_p^{(HD)} = 0.467$, and fewer $p\pi$ are formed than $d\pi$, just as expected from Fig. 2.

Some indication of the reliability of the present relative capture ratios may be obtained by comparison with previous work [1], which used the classical-trajectory Monte Carlo

_____

[1] This proportionality has no relationship to the energy-averaged constituent stopping powers, whose ratio has been shown experimentally [24] to be a poor indicator of relative capture (not surprising since stopping in the experimental target mainly depends on collisions at much higher energies than where capture occurs).
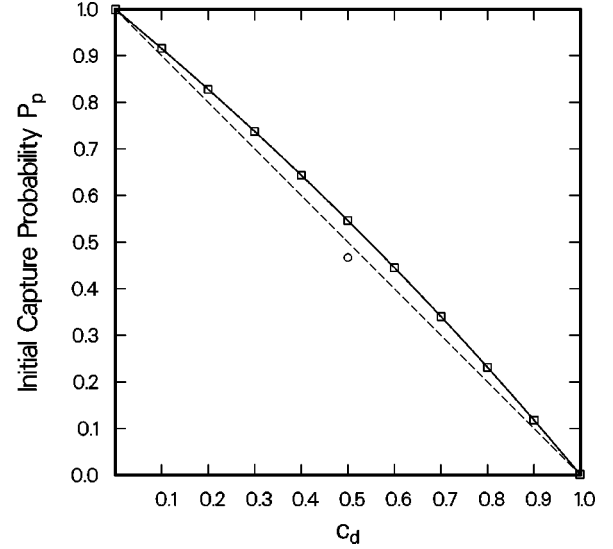
FIG. 6. Initial formation fraction P_p of $p\pi$ atoms, calculated using the FMD cross sections, as a function of deuterium fraction c_d. The squares are for the $H_2 + D_2$ mixture and the circle is for HD. The solid curve is a fit of the $H_2 + D_2$ points by $P_p^{(H_2+D_2)} = (1 - c_d)/(1 - 0.169 c_d)$, or equivalently $(P_p^{(H_2+D_2)}/P_d^{(H_2+D_2)})/(c_p/c_d) = 1.204$. The dashed line is the diagonal $P_p = c_p$.

(CTMC) method and explicitly calculated the arrival function for μ^- capture in a mixture of H and D *atoms*; in that work, $(P_d^{(H+D)}/P_p^{(H+D)})/(c_d/c_p) = 0.937$ was obtained, which may be compared with 0.923 obtained using the same CTMC capture cross sections but assuming a flat arrival function, and to 0.909 obtained using newly calculated FMD cross sections for the atomic targets and a flat arrival function. In all cases the dependence of the ratio on c_d was found to be very weak.

IV. COMPARISON WITH EXPERIMENTS AND INTERPRETATION

In a phenomenological description there are three distinct places where a c_d dependence of pion capture in a $H_2 + D_2$ mixture may arise. These are in the (1) pionic atom formation, (2) pion transfer, and (3) nuclear reaction. The nuclear reaction rate is significant only in a s state; however, this is usually not in a pure s state of an isolated atom but rather in a Stark-mixed state incurred during a collision with p or d. Thus, the accounting for all three physical processes is essentially atomic in nature.

For this model, the probability of the pion charge-exchange reaction with a proton in the $H_2 + D_2$ mixture was written [3]

$$W_{H_2D_2} = \left(\frac{k_p c_p}{k_p c_p + k_d c_d} \right) \left(\frac{\beta_{pp} c_p + \beta_{pd} c_d}{\beta_{pp} c_p + \beta_{pd} c_d + \lambda_{pd} c_d} \right)$$
$$+ \left(\frac{k_d c_d}{k_p c_p + k_d c_d} \right) \left(\frac{\lambda_{dp} c_p}{\beta_{dp} c_p + \beta_{dd} c_d + \lambda_{dp} c_p} \right), \qquad (21)$$

where

$$k_i c_i = \text{initial atomic capture on nucleus } i, \qquad (22a)$$

$\beta_{ij}c_j =$ nuclear absorption (facilitated by Stark mixing)

by i in collisions with j, (22b)

and

$\lambda_{ij}c_j =$ pion transfer from i to j. (22c)

The first term represents the fraction that is initially captured on p and does not subsequently transfer to d. The second term represents the fraction that is initially captured on d and transfers subsequently to p. Expression (21) assumes that (i) the pionic atom is formed before nuclear reaction occurs, (ii) the initial capture on species i is proportional to its concentration (verified in Sec. III B), (iii) a pion is not transferred more than once, and (iv) there is no density dependence (verified experimentally [25] — this means that radiation and processes having a nonlinear dependence on density are unimportant). But there are still too many parameters to be determined from the data. This expression can be significantly simplified by strengthening assumption (iii) and neglecting the second term. This additional approximation is considered justified since transfer from d to p is endothermic by $\gtrsim 9$ eV for $n \leq 5$. Although experiments have shown the existence of more energetic $p\pi$ atoms, they are probably not abundant enough to significantly affect the capture fractions.

The thus simplified expression can be parameterized as

$$W_{H_2D2} \approx \left(\frac{1}{1+\alpha C} \right) \left(\frac{1+\kappa C}{1+\kappa C + \Lambda C} \right),$$ (23)

where

$$\alpha \equiv k_d/k_p,$$ (24a)

$$\kappa \equiv \beta_{pd}/\beta_{pp},$$ (24b)

$$\Lambda \equiv \lambda_{pd}/\beta_{pp},$$ (24c)

and

$$C \equiv c_d/c_p.$$ (24d)

We have found that even the three parameters, α, κ, and Λ, are too correlated to be reliably determined from the experimental values of $W_{H_2D_2}$, measured for a wide range of C (or c_d) and shown in Fig. 7. There are various ways in which the data can be fit by essentially the same curve, obtained by varying just two of the parameters. However, which is used is not of purely academic interest since they imply different probabilities of pion transfer and this property is important in other contexts.

Although the data from the different experiments for π^- capture in $H_2 + D_2$ mixtures are in fairly good agreement, there appear to be small differences, perhaps due to normalization, that cause difficulties for the least-squares fits. For this reason, we have used only the points of Weber *et al.* [3] to determine the parameters. We present three fits, all of which give essentially the same χ^2 and are indistinguishable on the scale of Fig. 7, as follows.

(1) *Assume* $\alpha = 1$, as done in the original experimental analysis, and obtain (by least-squares fit) $\kappa = 1.46$ and Λ
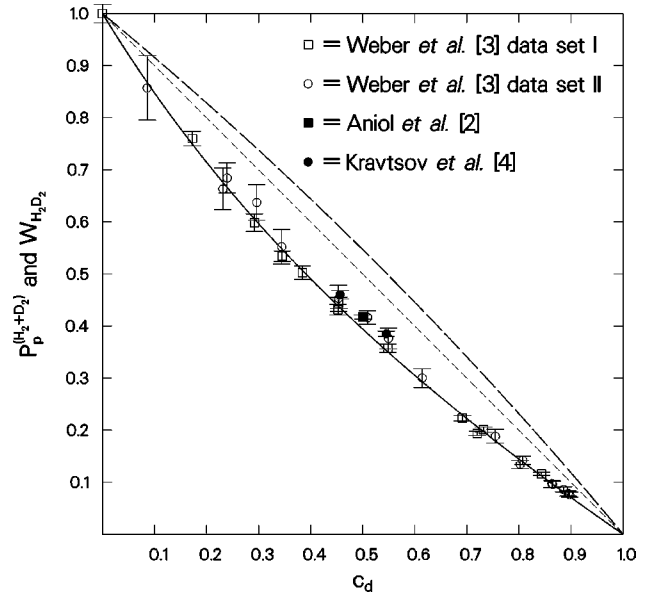
FIG. 7. Experimental data points [2–4] for *final* fraction $W_{H_2D_2}$ of $p\pi$ atoms (observed by π^- charge exchange with the proton) and their fit (solid curve) as a function of deuterium fraction c_d. Essentially the same fit (least squares using the Weber *et al.* [3] data points) is obtained by three different sets of parameters (see Table V). The long-dashed curve is the *initial* formation fraction $P_p^{(H_2+D_2)}$ and the short-dashed curve is the diagonal.

$=0.66$.[2] But we know that α is not really unity. The mainly kinematic difference found in the calculation of π^- capture in mixtures of the *atoms* H and D can be sensibly viewed as providing an upper limit $\alpha \lesssim 0.93$. Thus we consider this fit rather unphysical and a value of κ as large as found in this scenario unlikely.

(2) *Assume* $\kappa = 1$ in keeping with the theoretical expectation that Stark mixings in collisions with p or d are similar. They may differ principally because of their different relative velocities, which would suggest a slightly larger cross section for collisions with d since the Stark-mixing cross section is a decreasing function of velocity. However, in view of the convincing evidence from other experiments [21–23] that the pionic atoms are highly epithermal, this velocity effect will be diminished. With κ fixed at unity, we obtain $\alpha = 0.77$ and $\Lambda = 0.87$. This value of α is in reasonable agreement with the value 0.83 obtained using the FMD cross sections (see Sec. III B).

(3) *Fix* $\alpha = 0.83$, the present theoretical value, and then obtain $\kappa = 1.10$ and $\Lambda = 0.81$. This value of κ is not unreasonably large, and the isotope effect on Stark mixing, to the extent it exists, suggests $\kappa \gtrsim 1$.

The experiments [2–5] on pion capture in isotopic hydrogen mixtures were generally motivated and interpreted as determinations of the pion-transfer probability. Of course, deduction of the transfer probability Q required some as-

---

[2] These values are slightly different from the values $\kappa = 1.40$ and $\Lambda = 0.65$ given in Ref. [3]. This small difference is likely a result of their fit actually being done with numbers more precise than the three decimal places presented in Table I of Ref. [3]. A data point at $C = 5.295$ in data set I was omitted as recommended.
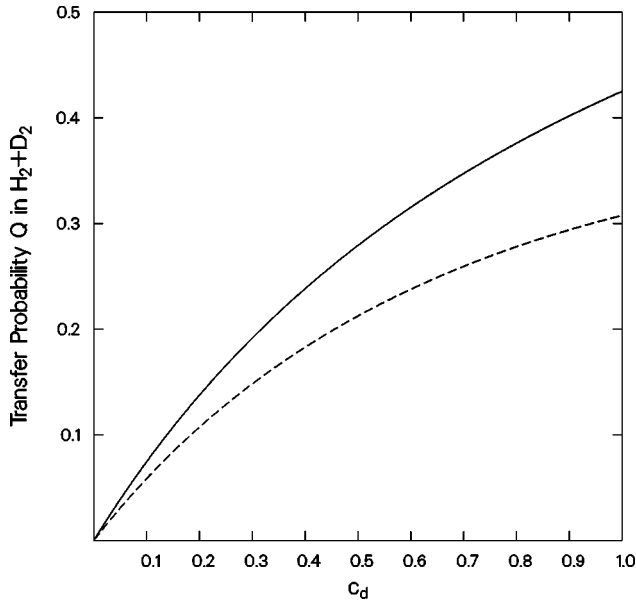
FIG. 8. Transfer probability Q [Eq. (25)] as a function of deuterium fraction c_d, deduced with the two different models. The dashed curve (fractional difference between the short-dashed and solid curves in Fig. 7) is that given using $P_p = c_p$ $(= 1 - c_d)$, as assumed in the experimental papers [3,5]. The solid curve (fractional difference between the long-dashed and solid curves in Fig. 7) is obtained using the presently calculated initial capture fractions P_p for a $H_2 + D_2$ mixture.

sumption about the initial capture probability and, for lack of better knowledge, it was taken as $P_p = c_p$. This assumption yields the dashed curve in Fig. 8. With our new knowledge of the initial capture, we can now reinterpret the data for $W_{H_2D_2}$ to obtain the transfer probability Q as a function of c_d,

$$Q = 1 - \frac{W_{H_2D_2}}{P_p^{(H_2+D_2)}} = \frac{\Lambda C}{1 + \kappa C + \Lambda C}, \qquad (25)$$

where the initial $p\pi$ formation fraction $P_p^{(H_2+D_2)}$ is given by Eq. (20) and the final (observed) $p\pi$ fraction $W_{H_2D_2}$ is given by Eq. (23) with parameters from Table V. This result is

TABLE V. Fits by Eq. (23) of experimental data [3]. The parameters are α = ratio d-to-p initial pion atomic capture, κ = ratio d-to-p Stark mixing of $p\pi$, and Λ = ratio transfer-to-Stark mixing. The χ^2/d.f. is for 27 degrees of freedom (29 data points, 2 parameters). Though the χ^2 are all essentially the same, fit 1 is considered unphysical; fit 3 may be slightly favored over fit 2 by theoretical predilection.

Fit no.	α	κ	Λ	χ^2/d.f.
1	1.00 [a]	1.46	0.66	1.171
2	0.77	1.00 [a]	0.87	1.156
3	0.83 [b]	1.10	0.81	1.160

[a]Fixed at unity.
[b]Fixed at theoretical value.

shown as the solid curve in Fig. 8. It is appreciably higher, 28% instead of 21% at $c_d = 0.5$, and 42% instead of 31% as $c_d \to 1$.

A different way to compare the present theory with experiments is to make side-by-side use of the data from the $H_2 + D_2$ and the HD experiments. On theoretical grounds, we expect pion (or muon) transfer from p to d to be similar in the two gases. The molecular effect, which could cause them to differ, has been shown theoretically to be small for ground-state muon transfer [26]; basically, this is because the exotic atom is small compared with the electronic molecule and momentum transfer between the exotic particle and electrons is inefficient. Pion transfer occurs mainly in excited states, but molecular effects should still be small for $n \approx 5$. Thus, the transfer can be expected to depend on the atomic fractions, c_p and c_d, but not much on the molecular arrangement of the atoms; for this reason the experimental data [2], which found proton capture $W_{H_2D_2}(c_d = 0.5) = 0.417 \pm 0.004$ but $W_{HD} = 0.338 \pm 0.008$, seemed very puzzling when the isotopic effect on initial capture was neglected. By comparing our theoretical *initial* capture fractions with these experimental *final* capture fractions, we can infer transfer probabilities of $23.7 \pm 0.7\%$ for the 50:50 $H_2 + D_2$ mixture and $27.6 \pm 1.7\%$ for HD gas (these error bars take into account only the stated experimental uncertainties), in satisfactory agreement. With the more recent Weber *et al.* [3] data for $W_{H_2D_2}$, we obtain 27.9% for transfer in 50:50 $H_2 + D_2$, as shown in Fig. 8, which is *the same as in* HD.

V. CONCLUSIONS

Molecular structure, taken into account by the FMD method, has large effects on the cross sections, initial quantum numbers, and kinetic energies for pionic atoms formed in collisions of negative pions with isotopic hydrogen molecules. The cross section for $p\pi$ formation in collisions with H_2 is larger than the cross section for $d\pi$ formation in collisions with D_2, but the probability of forming $d\pi$ is greater than the probability of forming $p\pi$ after pion capture by HD. These cross sections imply fractional formations of $p\pi$ and $d\pi$ that are significantly different for negative pions stopped in the 50:50 $H_2 + D_2$ gas mixture as opposed to HD gas. For the $H_2 + D_2$ mixtures, it is verified that the capture fractions are proportional, though not equal, to the isotopic fractions.

This knowledge, together with other experimental data [21–23] indicating that the $p\pi$ kinetic energies are epithermal and qualitative theoretical understanding of isotope effects on the Stark mixing cross sections, suggests a reinterpretation of the four existing experiments [2–5]. The three sets of parameters, given in Table V, all provide equally good fits of the experimental data. However, the first line, which corresponds to the original experimental analysis, can now reasonably be ruled out on the basis of (i) the theoretical initial capture fractions, (ii) inconsistency with the HD data, and (iii) the anomalously large isotope effect on the Stark mixing.

The most important quantity derived from the experimental data is the probability of pion transfer. In light of the properties of the pion cascade and nuclear absorption, it is expected that transfer mostly occurs in the excited levels $n = 4$ and 5, which are the same levels important to the q_{1s} factor in muon-catalyzed fusion [6,27]. The present results indicate that there is more transfer than previously believed.

With the calculated initial capture fractions in H_2+D_2 and HD, essentially the same pion p-to-d transfer rates are found to yield consistency with existing experimental data for H_2+D_2 mixtures and for HD.

[1] J. S. Cohen, R. L. Martin, and W. R. Wadt, Phys. Rev. A **27**, 1821 (1983).

[2] K. A. Aniol, D. F. Measday, M. D. Hasinoff, H. W. Roser, A. Bagheri, F. Entezami, C. Virtue, J. M. Stadlbauer, D. Horváth, M. Salomon, and B. C. Robertson, Phys. Rev. A **28**, 2684 (1983).

[3] P. Weber, D. S. Armstrong, D. F. Measday, A. J. Noble, S. Stanislaus, M. R. Harston, K. A. Aniol, and D. Horváth, Phys. Rev. A **41**, 1 (1990).

[4] A. V. Kravtsov, A. Yu. Mayorov, A. I. Mikailov, S. Yu. Ovchinnikov, N. P. Popov, V. M. Suvorov, and A. I. Shchetkovsky, Muon Catal. Fusion **2**, 199 (1988).

[5] V. I. Petrukhin and Yu. D. Prokoshkin, Zh. Éksp. Teor. Fiz. **56**, 501 (1969) [Sov. Phys. JETP **29**, 274 (1969)].

[6] B. Lauss *et al.*, Phys. Rev. Lett. **76**, 4693 (1996).

[7] J. Spuller *et al.*, Phys. Lett. **67B**, 479 (1977).

[8] R. MacDonald *et al.*, Phys. Rev. Lett. **38**, 746 (1977).

[9] M. Leon and H. A. Bethe, Phys. Rev. **127**, 636 (1962).

[10] J. S. Cohen, Phys. Rev. A **56**, 3583 (1997).

[11] J. S. Cohen, Phys. Rev. A **59**, 1160 (1999).

[12] J. S. Cohen, R. L. Martin, and W. R. Wadt, Phys. Rev. A **24**, 33 (1981).

[13] J. S. Cohen, Phys. Rev. A **27**, 167 (1983).

[14] J. S. Cohen, J. Phys. B **31**, L833 (1998).

[15] N. H. Kwong, J. D. Garcia, and J. S. Cohen, J. Phys. B **22**, L633 (1989).

[16] S. S. Gershtein, V. I. Petrukhin, L. I. Ponomarev, and Yu. D. Prokoshkin, Usp. Fiz. Nauk **97**, 3 (1969) [Sov. Phys. Usp. **12**, 1 (1970)].

[17] L. Wilets and J. S. Cohen, Contemp. Phys. **39**, 163 (1998).

[18] C. L. Kirschbaum and L. Wilets, Phys. Rev. A **21**, 834 (1980).

[19] J. S. Cohen, Phys. Rev. A **51**, 266 (1995); **57**, 4964 (1998).

[20] M. Leon, Phys. Rev. A **17**, 2112 (1978).

[21] J. F. Crawford, M. Daum, R. Frosch, B. Jost, P.-R. Kettle, R. M. Marshall, B. K. Wright, and K. O. H. Ziock, Phys. Lett. B **213**, 391 (1988); Phys. Rev. D **43**, 46 (1991).

[22] E. C. Aschenauer *et al.*, Phys. Rev. A **51**, 1965 (1995).

[23] A. Badertscher, M. Daum, R. Frosch, P. F. A. Goudsmit, W. Hajdas, M. Janousch, P.-R. Kettle, V. Markushin, J. Schottmüller, and Z. G. Zhao, Phys. Lett. B **392**, 278 (1997).

[24] A. V. Bannikov, B. Llévay, V. I. Petrukhin, V. A. Vasilyev, L. M. Kochenda, A. A. Markov, V. I. Medvedev, G. L. Sokolov, I. I. Strakovsky, and D. Horváth, Nucl. Phys. A **403**, 515 (1983).

[25] D. Horváth, Phys. Rev. A **30**, 2123 (1984).

[26] A. Adamczak (unpublished).

[27] M. Filipowicz, W. Czapliński, E. Guľa, A. Kravtsov, A. Mikhailov, and N. Popov, Nuovo Cimento D **20**, 155 (1998).